Hirvonen, V., Hammond, K., Chudyk, E., Limb, M., Spencer, J., Mulholland, A., & Van der Kamp, M. (2019). An Efficient Computational Assay for β-Lactam Antibiotic Breakdown by Class A β-Lactamases. *Journal of Chemical Information and Modeling*, *59*(8), 3365-3369. https://doi.org/10.1021/acs.jcim.9b00442

An efficient computational assay for β-lactam antibiotic breakdown by class A β-lactamases

Journal:	*Journal of Chemical Information and Modeling*
Manuscript ID	ci-2019-00442c.R1
Manuscript Type:	Letter
Date Submitted by the Author:	n/a
Complete List of Authors:	Hirvonen, Viivi; University of Bristol , School of Biochemistry Hammond, Katharine; University of Bristol, Centre for Computational Chemistry Chudyk, Ewa; University of Bristol, School of Chemistry Limb, Michael; University of Bristol, Centre for Computational Chemistry, School of Chemistry Spencer, James; University of Bristol, School of Cellular and Molecular Medicine Mulholland, Adrian; University of Bristol, School of Chemistry van der Kamp, Marc; University of Bristol, School of Biochemistry

An efficient computational assay for β-lactam antibiotic breakdown by class A β-lactamases

Viivi H. A. Hirvonen[a,b], Katharine Hammond[b#], Ewa I. Chudyk[b⊥], Michael A. L. Limb[b], James Spencer[c], Adrian J. Mulholland[b] and Marc W. van der Kamp[a,b*]

[a] School of Biochemistry, University of Bristol, University Walk, Bristol, BS8 1TD, UK; marc.vanderkamp@bristol.ac.uk, Tel: +44 117 331 2147.

[b] Centre for Computational Chemistry, School of Chemistry, University of Bristol, Cantock's Close, Bristol, BS8 1TS, UK.

[c] School of Cellular and Molecular Medicine, University of Bristol, University Walk, Bristol, BS8 1TD, UK.

Supporting Information Placeholder

ABSTRACT: Class A β-lactamases cause clinically relevant resistance to β-lactam antibiotics. Carbapenem degradation is a particular concern. We present an efficient QM/MM molecular simulation protocol that accurately predicts the activity of β-lactamases against carbapenems. Simulations take <24 CPU hours, a >99% reduction, and do not require fitting against experimental data or significant parameterization. This computational assay also reveals mechanistic details of β-lactam breakdown and should assist in evaluating emerging β-lactamase variants and developing new antibiotics.

Antibiotic resistance is one of the most concerning phenomena of the 21st century.[1, 2] To some extent, this resistance occurs naturally, but in recent decades its spread has been accelerated by the excessive use of antibiotics.[3] β-lactam drugs are one of the largest groups of commercially available antibiotics and they remain the most prescribed ones,[4] but they also suffer from increasing clinical resistance.[5] The most important causes for this resistance, especially in Gram-negative bacteria, are the β-lactamase enzymes.[6-8]

β-lactamases can be divided into four different classes based on their primary amino acid sequence homology (Ambler classification): classes A, C, and D are serine β-lactamases with an active site serine residue, whilst class B are metallo-β-lactamases with active site zinc ion(s).[9] Of the four classes class A β-lactamases are the largest, with many clinically significant enzymes. They can inactivate a broad range of β-lactam substrates: in addition to hydrolyzing penicillins and cephalosporins, some family members can also mediate resistance against carbapenems.[10-12] Carbapenems are mainly used as 'last resort' antibiotics or for difficult infections,[13] hence the Centers for Disease Control and Prevention (CDC) have categorized the clinical importance of carbapenemase-producing Enterobacteriaceae (the group of Gram-negative bacteria including *Escherichia coli* and *Klebsiella pneumoniae*) as "an immediate public health threat that requires urgent and aggressive action".[14]

β-lactamases inactivate β-lactam antibiotics by hydrolyzing the β-lactam amide (Figure 1). In serine β-lactamases, this consists of two consecutive reactions: acylation, resulting in formation of a covalently-bound acylenzyme, and deacylation.[8] In acylation, a nucleophilic attack by the active site serine upon the β-lactam carbonyl carbon occurs to form the acylenzyme, via a tetrahedral intermediate.[15] Deacylation is analogous to acylation including a tetrahedral intermediate (TI), but the nucleophile is an active site water molecule (the deacylating water, DW). In class A enzymes, both nucleophiles are activated via proton abstraction by an active site glutamate residue (Glu166 in the class A β-lactamase numbering scheme).[16, 17] β-lactamases are typically inhibited when the acylenzyme intermediate is long-lived due to slow deacylation rates.[18] For many β-lactam:β-lactamase combinations, in particular reactions involving carbapenems, TI formation in deacylation of the acylenzyme is probably the rate-limiting step.[13] Therefore, to determine the carbapenemase activity of class A β-lactamases, only this reaction needs to be modelled.

Previously, a quantum mechanics/molecular mechanics (QM/MM) protocol for modelling TI formation in the deacylation step for class A enzymes with meropenem was shown to correctly distinguish between carbapenemases and non-carbapenemases.[18] Using the proposed protocol, carbapenem-inhibited enzymes showed deacylation barriers of 17.0-18.9 kcal/mol, whilst for carbapenem-hydrolyzing enzymes the values were 7.5-10.5 kcal/mol. A similar computational protocol has been used to study class A β-lactamase inhibition by clavulanate, which identified the covalent clavulanate complex responsible for irreversible β-lactamase inhibition.[19] Being based on QM methods and standard force fields, no additional parameterization is required for their application. Despite the promising results of these protocols, the carbapenem assay requires significant computational resources due to extensive sampling of the free energy surface. Hence, it cannot be used for more rapid, computationally efficient, screening of a variety of different enzyme-antibiotic combinations.

Starting from our previous work, here we present and validate a more rapid computational assay that can discriminate between carbapenemase activities using only limited computational resources. The resources are minimized first by limiting the area on the free energy surfaces (FES) to be sampled, and then by reducing the sampling time. We demonstrate that this reduced protocol, requiring less than 1 % of the computational resources of the

original assay, can still correctly distinguish between carbapenemases and carbapenem-inhibited class A β-lactamases. It therefore provides an efficient computational diagnostic towards *in silico* screening of β-lactamase activity.

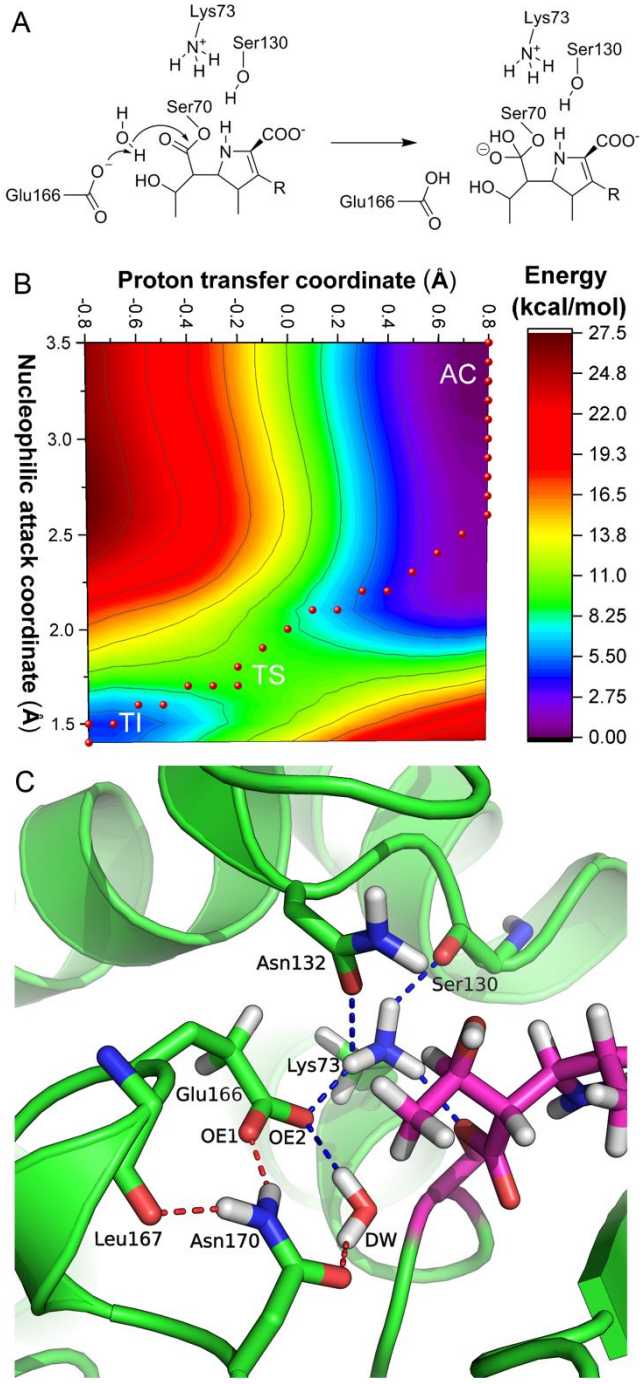

Figure 1. A) First step of deacylation in class A β-lactamases. Glu166 acts as a proton acceptor allowing the deacylating water to perform nucleophilic attack on the acylenzyme, which results in tetrahedral intermediate formation. B) Full free energy surface of deacylation for KPC-2 with meropenem. Red circles show the positions of umbrella sampling windows along the approximate "standard" minimum free energy path (MFEP) used for all enzymes. AC = acylenzyme, TS = approximate transition state, TI = tetrahedral intermediate**.** C) Active site of KPC-2 highlighting the hydrogen bonds between Glu-166 OE1 and OE2 and relevant residues. Meropenem in magenta.

We investigate eight class A β-lactamases, including the widely distributed *K. pneumoniae* carbapenemase (KPC), and the TEM, SHV and CTX-M enzymes (Table 1), selected for their clinical relevance and their ability (or inability) to hydrolyse carbapenems. Acylenzyme systems were prepared as described previously (details in ESI).[18] Briefly, structures were solvated in water and minimized, followed by heating to 300 K in 50 ps. Starting structures for umbrella sampling (US) were then taken after at least 50 ps of unrestrained QM/MM MD (with starting points for repeat simulations at least 15 ps apart). Two reaction coordinates are used for umbrella sampling: one for the proton transfer between DW and Glu166, and one the nucleophilic attack of DW on the acylenzyme carbonyl. The DFTB2 (SCC-DFTB) method was used for the QM region.[20] All calculations were performed with sander from AmberTools16.[21] The weighted-histogram analysis method (WHAM)[22] was used to analyze US results and to obtain calculated barriers for each reaction ($\Delta^{\ddagger}G_{calc}$). Three independent US simulations were run for each acylenzyme to test convergence of $\Delta^{\ddagger}G_{calc}$ (details in the ESI; meropenem parameters at DOI 10.6084/m9.figshare.8158097).

Several modifications to the protocol were evaluated in order to improve computational efficiency. First, the amount of sampling was reduced by sampling only at those US windows corresponding to the approximate minimum free energy path (MFEP) on the FES. Based on our earlier work,[18] the calculated MFEPs on full FESs across all eight studied β-lactamases are similar, which implies that only a partial FES needs to be calculated to compare the deacylation rates between studied enzymes. The "standard" MFEP used for partial sampling along the FES is presented in Figure 1 (and in the ESI). Sampling only in windows along this MFEP reduces the amount of US calculations from the original 374 to 28 per (partial) surface. The more limited sampling along the surface does not change the resulting $\Delta^{\ddagger}G_{calc}$ values significantly (which are underestimated at this QM level, as expected[18]), with the largest calculated change between full and partial surface calculations being 2.5 kcal/mol (Table 1). Despite some changes in $\Delta^{\ddagger}G_{calc}$ values for all enzymes, the correct division into two groups is maintained. Carbapenemases (KPC, SFC, SME and NMC) have $\Delta^{\ddagger}G_{calc}$ values between 7.8-10.4 kcal/mol, and carbapenem-inhibited enzymes (SHV, TEM, BlaC and CTX-M) between 15.5-16.8 kcal/mol. This suggests that the standard MFEP describes deacylation sufficiently well for differentiating between different carbapenem-hydrolyzing abilities.

Even when the amount of US windows is significantly reduced, the computational time for each window remains high. Hence, the possibility of utilizing shorter sampling times was first tested using the original 20 ps US results. This was done by using only the first 0.5, 1, 2, 5 or 10 ps of each 20 ps US window to calculate $\Delta^{\ddagger}G_{calc}$ values (Table S2). This differs from sampling each window for a shorter time only, since the system is still allowed to equilibrate for 20 ps before changing the reaction coordinate restraints. Nonetheless, this preliminary analysis can be used to study the effects of shorter sampling. The results indicate that sampling for only a fraction of 20 ps is enough to distinguish between the two groups of β-lactamases. In most cases, the preliminary shorter sampling times yield somewhat higher barriers (<2.5 kcal/mol), which is expected due to reduced sampling of the phase space. However, this does not affect the distinction between carbapenemases and non-carbapenemases. When reducing sampling to 1 ps per window or less, more significant increases of the barrier heights (up to 20%) become common. We thus decided

to use 2 ps US sampling per window. Sampling for 2 ps also ensures enough overlap between sampling in adjacent US windows.

Table 1. Comparison of experimental ($\Delta^{\ddagger}G_{exp}$) and calculated free energies of activation ($\Delta^{\ddagger}G_{calc}$) for the first step of deacylation of meropenem by eight enzymes using different protocols.

β-lactamase	k_{cat} (s^{-1}) [a]	$\Delta^{\ddagger}G_{exp}$ (kcal/mol) [b]	$\Delta^{\ddagger}G_{calc}$ (kcal/mol) [c]		
			Full [a]	MFEP (20ps)	MFEP (2ps)
KPC-2	3.6	16.8	10.5 (0.9)	8.5 (2.2)	9.1 (1.1)
SFC-1	6.5	16.6	10.9 (0.9)	10.4 (1.2)	9.9 (1.3)
SME-1	3.2	16.9	10.3 (2.8)	7.8 (0.2)	9.5 (1.4)
NMC-A	12.0	16.1	7.5 (0.4)	8.8 (0.4)	10.4 (0.7)
SHV-1	0.0013	21.6	17.0 (0.4)	16.1 (1.0)	19.5 (0.5)
TEM-1	0.0023	22.7	17.1 (0.4)	16.3 (2.2)	23.6 (1.4)
BlaC	0.0017	21.5	17.9 (0.1)	15.5 (2.2)	24.7 (1.1)
CTX-M-16	0.0042	20.8	18.9 (1.1)	16.8 (1.5)	17.2 (1.6)
Computer resource (%) [d]			100	7.5	0.75

a) Values taken from ref. 19. b) Calculated from experimental rate constants using the Eyring equation, see ref. 19. c) Barriers are calculated from three simulations using WHAM as described in the ESI, standard deviations in parenthesis. d) Computer resources required are estimated by extrapolating the time needed for all required QM/MM (DFTB2/ff12SB) simulations from 2 ps calculations: 374 umbrella sampling windows for the whole surface and 20 ps per window (374 x 20) for "Full", 28 windows x 20 ps for "MFEP (20ps)" and 28 windows x 2 ps for "MFEP (2ps)".

Sampling for only 2 ps per window along the MFEP gives similar overall results to sampling for 20 ps (Table 1). With the shorter protocol, carbapenemases have $\Delta^{\ddagger}G_{calc}$ values of 9.1-10.4 kcal/mol, whilst carbapenem-inhibited enzymes have $\Delta^{\ddagger}G_{calc}$ values of 17.2-24.7 kcal/mol. Shorter US gives higher deacylation $\Delta^{\ddagger}G_{calc}$ values for all enzymes when compared to calculations using 20 ps sampling along the MFEP, with most significant increases seen for carbapenem-inhibited enzymes (0.4-9.2 kcal/mol). However, the increased deacylation barriers do not change the division of the enzymes into the two distinct groups. Furthermore, the shortened protocol (see ESI for details) enables running calculations on modest computing resources (e.g. on a desktop with one CPU) in a reasonable time. For the largest system (SFC-1, containing 54.9k atoms), US takes on average 23 hours to finish on one 2.6 GHz CPU. In general, the more efficient assay requires less than 1 % of the computer resources needed for the original assay (Table 1).

The efficient assay we have developed can be used to study specific mechanistic details of carbapenem hydrolysis. Glu166, the general base in deacylation, has two chemically inequivalent carboxylate oxygens: one that forms a hydrogen bond with Asn170 (OE1), and one that interacts with Lys73 (OE2) (Figure 1C). The DW hydrogen bonds with OE2 in all MD simulations, and the US calculations have been performed using this oxygen as the proton acceptor. However, proton transfer to OE1 might also be relevant for deacylation. We thus used our new, efficient protocol to compare the two possible proton acceptors. When forcing the proton transfer to OE1, the $\Delta^{\ddagger}G_{calc}$ values increase by >3 kcal/mol for the carbapenemases (Table S3). Significant increases also incur for the carbapenem-inhibited enzymes (especially if the barrier with proton transfer to OE2 was not very high already). This consistent increase implies that the most probable proton transfer pathway in carbapenem hydrolysis is via Glu166:OE2 that interacts with Lys73, thus indicating an important role for this residue.

Preference for one carboxylate oxygen (where the two oxygens have different hydrogen bonding environments) as the general base has been observed also in other enzymes.[23] For the β-lactamases here, the DW is primarily hydrogen bonded with OE2 in the acylenzyme MD simulations and this interaction is thus present in all starting structures for US calculations. The preference for OE2 acting as the base can be explained by inspecting the additional hydrogen bonds formed by the Lys73 and Asn170 side chains. Lys73 interacts with Glu166:OE2 as well as Asn132, Ser70, meropenem and the Ser130 backbone carbonyl oxygen, whilst Asn170 interacts only with Glu166:OE1 and the backbone carbonyl of Leu167. Upon a proton transfer, other residues can balance the weakening interaction of Lys73 with Glu166:OE2, whereas Asn170 has fewer other interactions for such stabilization.

In conclusion, the carbapenemase activity of eight class A β-lactamases was assayed *in silico* using QM/MM reaction simulations with an optimized, efficient computational protocol. Assays based on computational biomolecular simulation are increasingly common and can complement traditional experimental assays.[24] Assay efficiency is achieved here by using the semi-empirical DFTB2 method and by limiting both conformational space and time sampled. Distinction between four enzymes known to efficiently hydrolyse carbapenems, and four enzymes that do not, can be made within a day with very modest computer resources (e.g. one CPU per enzyme). Additionally, this efficient assay can be used to inspect mechanistic aspects of carbapenem inactivation; exemplified here by comparing the $\Delta^{\ddagger}G_{calc}$ values of the first deacylation step for two possible proton transfer pathways. The short computational assay time with moderate computer resources now makes this assay attractive for more rapid *in silico* activity screening of different class A β-lactamase – antibiotic combinations. This will assist assessment and understanding of resistance to β-lactam drugs as conferred by β-lactamases, e.g. the effect of acquired point mutations on drug hydrolysis. As access to genome sequences of pathogen isolates becomes more routine, such information could be used in guiding prescription decisions.

Furthermore, elucidation of mechanistic details of acyl-enzyme hydrolysis, as identified in simulations, may guide the development of new β-lactams or β-lactamase inhibitors designed to evade the activity of broad-spectrum and carbapenem-hydrolyzing β-lactamases.

ASSOCIATED CONTENT

Supporting Information. Simulation details including system setup, all steps of the efficient computational assay, WHAM analysis and energies for the alternative proton transfer reaction.

AUTHOR INFORMATION

Corresponding Author

*Email: marc.vanderkamp@bristol.ac.uk

Present addresses

[#] National Physical Laboratory, Hampton Road, Teddington, Middlesex, TW11 0LW, UK & Department of Physics and Astronomy, University College London, London, WC1E 6BT, UK. [⊥] Vertex Pharmaceuticals (Europe) Ltd., 86-88 Jubilee Ave, Milton Park, Abingdon-on-Thames, OX14 4RW, UK.

Author Contributions

MWK and AJM designed the study; VHAH, MWK, KH, EIC and MALL performed and analyzed all simulations, supervised by AJM and MWK. VHAH, KH, JS, AJM and MWK contributed to writing the manuscript.

ACKNOWLEDGMENT

This work was supported in part by grant MR/N0137941/1 for the GW4 Biomed DTP (VHAH), awarded to the Universities of Bath, Bristol, Cardiff and Exeter from the Medical Research Council (MRC). MWK is a BBSRC David Phillips Fellow (BB/M026280/1). MALL thanks BBSRC and Pfizer for support. EIC (EP/G007705/1), AJM (EP/M022609/1, EP/M027546/1, EP/G007705/1) and JS (EP/M027546/1) thank EPSRC for support. This work was conducted using the computational facilities of the Advanced Computing Research Centre, University of Bristol.

References

1. Zaman, S. B.; Hussain, M. A.; Nye, R.; Mehta, V.; Mamun, K. T.; Hossain, N. A Review on Antibiotic Resistance: Alarm Bells are Ringing. *Cureus* **2017,** *9*, e1403.
2. Fair, R. J.; Tor, Y., Antibiotics and Bacterial Resistance in the 21st Century. *Perspect. Medicin. Chem.* **2014,** *6*, 25-64.
3. Davies, J.; Davies, D., Origins and Evolution of Antibiotic Resistance. *Microbiol. Mol. Biol. Rev.* **2010,** *74*, 417-433.
4. Klein, E. Y.; Van Boeckel, T. P.; Martinez, E. M.; Pant, S.; Gandra, S.; Levin, S. A.; Goossens, H.; Laxminarayan, R. Global Increase and Geographic Convergence in Antibiotic Consumption Between 2000 and 2015. *Proc. Natl. Acad. Sci. U S A* **2018,** *115*, E3463-E3470.
5. Worthington, R. J.; Melander, C. Overcoming Resistance to beta-Lactam Antibiotics. *J. Org. Chem.* **2013,** *78*, 4207-4213.
6. Munita, J. M.; Arias, C. A. Mechanisms of Antibiotic Resistance. *Microbiol. Spectr.* **2016,** *4*.
7. Bush, K. Alarming beta-Lactamase-mediated Resistance in Multidrug-resistant Enterobacteriaceae. *Curr. Opin. Microbiol.* **2010,** *13*, 558-564.
8. Tooke, C. L.; Hinchliffe, P.; Bragginton, E. C.; Colenso, C. K.; Hirvonen, V. H. A.; Takebayashi, Y.; Spencer, J. beta-Lactamases and beta-Lactamase Inhibitors in the 21st Century. *J. Mol. Biol.* **2019**.
9. Ambler, R. P. The Structure of beta-Lactamases. *Phil. Trans. R. Soc. Lond. B* **1980,** *289*, 321-331.
10. Queenan, A. M.; Bush, K. Carbapenemases: the Versatile beta-Lactamases. *Clin. Microbiol. Rev.* **2007,** *20*, 440-458.
11. Pfeifer, Y.; Cullik, A.; Witte, W. Resistance to Cephalosporins and Carbapenems in Gram-negative Bacterial Pathogens. *Int. J. Med. Microbiol.* **2010,** *300*, 371-379.
12. Drawz, S. M.; Bonomo, R. A., Three Decades of beta-Lactamase Inhibitors. *Clin. Microbiol. Rev.* **2010,** *23*, 160-201.
13. Papp-Wallace, K. M.; Endimiani, A.; Taracila, M. A.; Bonomo, R. A. Carbapenems: Past, Present, and Future. *Antimicrob. Agents. Chemother.* **2011,** *55*, 4943-4960.
14. Centers for Disease Control. Antibiotic Resistance Threats in the United States, 2013. https://www.cdc.gov/drugresistance/threat-report-2013/pdf/ar-threats-2013-508.pdf (accessed 10/01).
15. Hermann, J. C.; Pradon, J.; Harvey, J. N.; Mulholland, A. J., High Level QM/MM Modeling of the Formation of the Tetrahedral Intermediate in the Acylation of Wild Type and K73A Mutant TEM-1 Class A Beta-Lactamase. *J. Phys. Chem. A* **2009,** *113*, 11984-11994.
16. Minasov, G.; Wang, X.; Shoichet, B. K., An Ultrahigh Resolution Structure of TEM-1 beta-lactamase Suggests a Role for Glu166 as the General Base in Acylation. *J. Am. Chem. Soc.* **2002,** *124*, 5333-5340.
17. Hermann, J. C.; Ridder, L.; Holtje, H. D.; Mulholland, A. J. Molecular Mechanisms of Antibiotic Resistance: QM/MM Modelling of Deacylation in a Class A beta-Lactamase. *Org Biomol Chem* **2006,** *4*, 206-210.
18. Chudyk, E. I.; Limb, M. A.; Jones, C.; Spencer, J.; van der Kamp, M. W.; Mulholland, A. J. QM/MM Simulations as an Assay for Carbapenemase Activity in Class A beta-Lactamases. *Chem. Commun.* **2014,** *50*, 14736-14739.
19. Fritz, R. A.; Alzate-Morales, J. H.; Spencer, J.; Mulholland, A. J.; van der Kamp, M. W., Multiscale Simulations of Clavulanate Inhibition Identify the Reactive Complex in Class A beta-Lactamases and Predict the Efficiency of Inhibition. *Biochemistry* **2018,** *57*, 3560-3563.
20. Elstner, M.; Frauenheim, T.; Kaxiras, E.; Seifert, G.; Suhai, S. A Self-Consistent Charge Density-Functional Based Tight-Binding Scheme for Large Biomolecules. *Phys. Stat. Sol.* **2000,** *217*, 357-376.
21. Case, D. A.; Cerutti, D. S.; Cheatham, T. E. I.; Darden, T. A.; Duke, R. E.; Giese, T. J.; Gohlke, H.; Goetz, A. W.; Greene, D.; Homeyer, N.; Izadi, S.; Kovalenko, A.; Lee, T. S.; LeGrand, S.; Li, P.; Lin, C.; Liu, J.; Luchko, T.; Luo, R.; Mermelstein, D.; Merz, K. M.; Monard, G.; Nguyen, H.; Omelyan, I.; Onufriev, A.; Pan, F.; Qi, R.; Roe, D. R.; Roitberg, A.; Sagui, C.; Simmerling, C. L.; Botello-Smith, W. M.; Swails, J.; Walker, R. C.; Wang, J.; Wolf, R. M.; Wu, X.; Xiao, L.; York, D.M; Kollman, P.A. *AMBER 2017*, University of California: San Francisco, 2017.
22. Kumar, S.; Bouzida, D.; Swendsen, R. H.; Kollman, P. A.; Rosenberg, J. M. The Weighted Histogram Analysis Method for Free-Energy Calculations on Biomolecules. I. The Method. *J. Comput. Chem.* **1992,** *13*, 1011-1021.
23. Masgrau, L.; Ranaghan, K. E.; Scrutton, N. S.; Mulholland, A. J.; Sutcliffe, M. J. Tunneling and Classical Paths for Proton Transfer in an Enzyme Reaction Dominated by Tunneling: Oxidation of Tryptamine by Aromatic Amine Dehydrogenase. *J. Phys. Chem. B* **2007,** *111*, 3032-3047.

24. Huggins, D. J.; Biggin, P. C.; Dämgen, M. A.; Essex, J. W.; Harris, S. A.; Henchman, R. H.; Khalid, S.; Kuzmanic, A.; Laughton, C. A.; Michel, J.; Mulholland, A. J.; Rosta, E.; Sansom, M. S. P.; van der Kamp, M. W., Biomolecular simulations: From dynamics and mechanisms to computational assays of biological activity. *Wiley Interdisciplinary Reviews: Computational Molecular Science* **2019,** *9*, e1393.

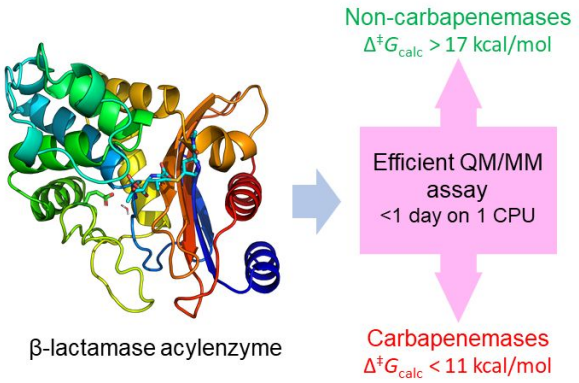

For Table of Contents Only

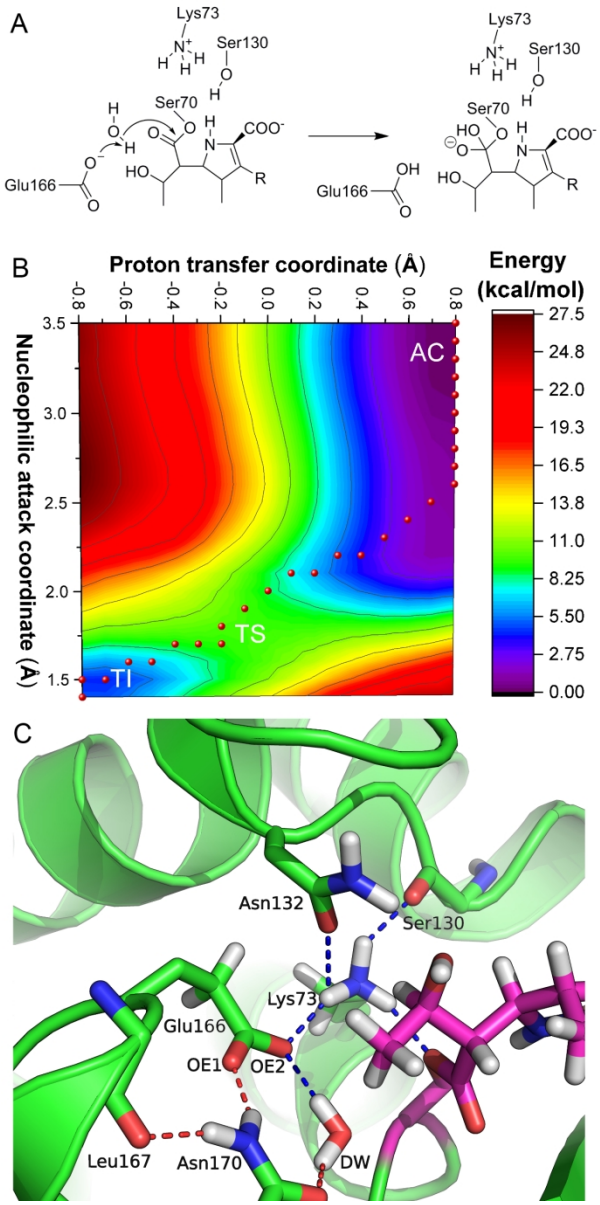

Figure 1. A) First step of deacylation in class A β-lactamases. Glu166 acts as a proton acceptor allowing the deacylating water to perform nucleophilic attack on the acylenzyme, which results in tetrahedral intermediate formation. B) Full free ener-gy surface of deacylation for KPC-2 with meropenem. Red circles show the positions of umbrella sampling windows along the approximate "standard" minimum free energy path (MFEP) used for all enzymes. AC = acylenzyme, TS = approx-imate transition state, TI = tetrahedral intermediate. C) Active site of KPC-2 highlighting the hydrogen bonds between Glu-166 OE1 and OE2 and relevant residues. Meropenem in magenta.

109x219mm (300 x 300 DPI)

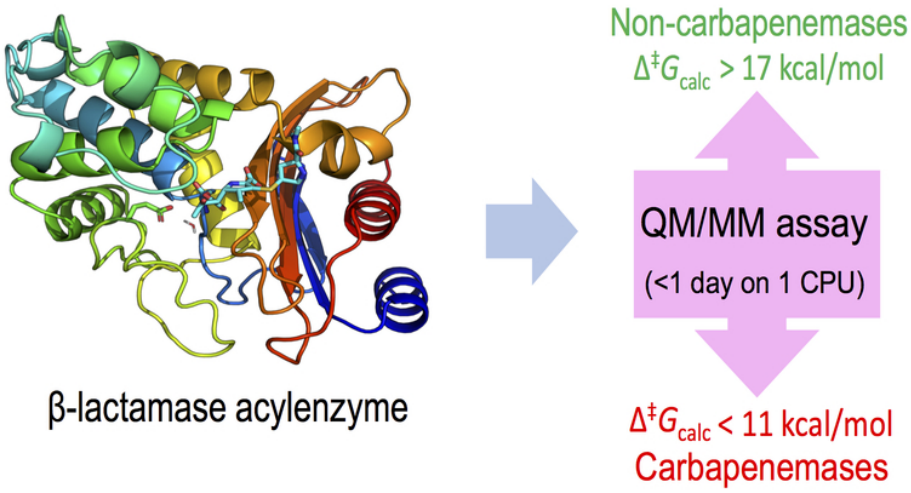

TOC graphic

69x37mm (300 x 300 DPI)